versity where he is a Professor at the Research Institute of Electronics. He has worked on milimeter-wave magnetrons, gigabit-pulse regenerators, solid-state oscillators, and device-circuit interaction problems. His current research interests are concerned with microwave power-combining techniques, microwave thermography, and medical electronics.

Dr. Mizushina is a member of the Institute of Electronics and Communication Engineers of Japan, the Japan Society of Medical Electronics and Biological Engineering, and Sigma Xi.

Transversely Anisotropic Optical Fibers: Variational Analysis of a Nonstandard Eigenproblem

ISMO V. LINDELL, SENIOR MEMBER, IEEE MARKKU I. OKSANEN, STUDENT MEMBER, IEEE

Abstract—**The variational principle for nonstandard eigenvalue problems, recently reported by one of the authors, is applied for the study of guided-wave propagation in an anisotropic dielectric waveguide. A stationary functional is derived for the general dielectric waveguide with transverse anisotropy. The functional is tested for the well-known case of an isotropic step-index single-mode fiber. It is seen that for simple trial functions with only two parameters, a good accuracy is obtained. For two types of transversely anisotropic step-index fibers, relations between the propagation factor, anisotropy parameter, dielectric parameter, and frequency are calculated. The functional does not assume weak guidance condition nor perturbational anisotropy and, hence, is also applicable for other dielectric waveguides. In this application, only a modest computer or a programmable calculator is needed. Moreover, the spurious modes causing confusion in the finite-element method of calculation do not appear with the present method.**

I. Introduction

The OPTICAL FIBER has become one of the most studied subjects in electromagnetics because of its phenomenological property of wave guidance with extremely low losses. In recent years, the single-mode fiber has been favored because of its small dispersion, but the problem has been the degeneracy in the polarization of the basic HE_{11} mode in fibers with circular symmetry. Because of this, the small imperfections in the ambient conditions of the fiber have the effect of making the polarization of the mode a statistically varying quantity after a few meters of propagation in the fiber [1]–[5], a fact that has been counteracted by producing noncircular or transversely anisotropic fibers. By analysis and actual fabrication, it has been shown that the noncircularity in most cases is insufficient to produce the required separation of the polarization degenerate mode propagation coefficients, whereas by introducing mechanical stress in the fiber, an anisotropy can be obtained high enough to produce a separation sufficient in practice [3], [6]–[17]. This motivates an analysis of the dielectric waveguide with transverse anisotropy, because although the longitudinal anisotropy has been well studied [18]–[21], there only exist a few attempts with more general anisotropy: mainly perturbational or dealing with special structures [22]–[26].

The analysis applies the variational principle in the general eigenvalue problem which was called nonstandard in a recent study by one of the authors [27]. Here, the problem can be expressed in abstract operator form as

$$L(\lambda)f=0 \tag{1}$$

where λ is the eigenvalue parameter of the problem. If $L(\lambda)$ is a linear function on λ, (1) is a standard eigenvalue problem, otherwise it is called nonstandard. The parameter λ may be chosen at will among all the physical and geometrical parameters involved in the problem. In problems dealing with closed waveguides, there is an additional equation corresponding to boundary conditions, which, however, is absent in our present problem. The method is based on the following functional equation obtained through definition of an inner product (.,.):

$$(f, L(\lambda)f)=0. \tag{2}$$

If the operator L is self adjoint with respect to this inner product, it was shown that (2) possesses stationary roots for the parameter λ [27]. If we can solve (2) for λ, a stationary functional for λ is obtained, which can be applied for an approximative solution of the problem (1) in a well-known manner [28]. In more complicated problems, however, no explicit solution of (2) for the parameter λ can be found. In this case, we may try to take another parameter of the problem as our eigenvalue parameter λ. If none

Manuscript received November 12, 1982; revised May 3, 1983. This work was supported by a grant from the Academy of Finland.

The authors are with the Electrical Engineering Department, Helsinki University of Technology, Otakaari 5A, Espoo 15, Finland 02150.

0018-9480/83/0900-0736$01.00 ©1983 IEEE

of the parameters is solvable from (2) in explicit form, we can define new parameters out of the old ones and try to solve (2) for one of them. It is self-evident that this also leads to a stationary functional, because, if in the original problem (1) the parameters are redefined, a functional equation (2) with a new set of parameters arises. Hence, the change of parameters can also be made in (2).

In Section II, the nonstandard equation (1) is derived for longitudinal field components, leading to a self-adjoint problem, which is of the nonstandard form in all parameters. By defining new independent parameters, an explicit stationary functional can be written for the parameter ω^2. In Section III, the functional is tested for the step-index isotropic fiber. It is seen that for a two-parameter test function, a good accuracy is obtained for the dispersion relation. In Section IV, the functional is applied to two types of transversely anisotropic fibers: one with an anisotropic core and an isotropic cladding and the other with both the core and cladding anisotropic, and relations between different parameters are calculated. Because the method is very general, and also boundary conditions could be introduced as in a previous study [29] for isotropic waveguides, the present procedure can be applied to other waveguide structures with anisotropic media.

II. Theory

We consider a dielectric guiding structure with dyadic permittivity inhomogeneous in the $x-y$ plane. The ϵ dyadic is supposed to possess the guiding direction unit vector $\boldsymbol{u}$ $(=\boldsymbol{u}_z)$ as its eigenvector so that we have

$$\epsilon(\rho)\cdot\boldsymbol{u}=\epsilon_u(\rho)\boldsymbol{u}. \tag{3}$$

Moreover, ϵ is assumed to be a symmetric dyadic, as is the case for crystal media. Henceforth, we write $\epsilon(\rho)+\epsilon_u(\rho)\boldsymbol{uu}$ instead of $\epsilon(\rho)$, or boldface $\boldsymbol{\epsilon}$ denotes the two-dimensional part of the permittivity tensor.

Analogously with [29], we derive equations for the longitudinal fields. In fact, writing the guided fields as $\boldsymbol{E}(\boldsymbol{r})=(\boldsymbol{e}(\rho)+\boldsymbol{u}e(\rho))\ \exp(-j\beta z)$ and $\boldsymbol{H}(\boldsymbol{r})=(\boldsymbol{h}(\rho)+\boldsymbol{u}h(\rho))\ \exp(-j\beta z)$, from Maxwell's equations we have

$$\nabla\cdot(\boldsymbol{u}\times\boldsymbol{e})-j\omega\mu h=0 \tag{4}$$

$$\nabla\cdot(\boldsymbol{u}\times\boldsymbol{h})+j\omega\epsilon_u e=0 \tag{5}$$

$$\boldsymbol{u}\times\nabla e+j\beta\boldsymbol{u}\times\boldsymbol{e}-j\omega\mu\boldsymbol{h}=0 \tag{6}$$

$$\boldsymbol{u}\times\nabla h+j\beta\boldsymbol{u}\times\boldsymbol{h}+j\omega\boldsymbol{\epsilon}\cdot\boldsymbol{e}=0. \tag{7}$$

From these equations, the transversal field vectors $\boldsymbol{e}$, $\boldsymbol{h}$ can be eliminated. Equations (6) and (7), then, give us

$$\boldsymbol{e}=-j\boldsymbol{k}_c^{-2}\cdot(\beta\nabla e-\omega\mu\boldsymbol{u}\times\nabla h) \tag{8}$$

$$\boldsymbol{h}=j\boldsymbol{u}\times\boldsymbol{k}_c^{-2}\cdot(-\omega\boldsymbol{\epsilon}\cdot\nabla e+\beta\boldsymbol{u}\times\nabla h) \tag{9}$$

if we define

$$\boldsymbol{k}_c^2=\omega^2\mu\boldsymbol{\epsilon}-\beta^2\boldsymbol{E} \tag{10}$$

where $\boldsymbol{E}$ is the two-dimensional unit dyadic $\boldsymbol{E}=\boldsymbol{I}-\boldsymbol{uu}$. The dyadic $\boldsymbol{k}_c^2$ is two-dimensional and because $\det(\boldsymbol{k}_c^2)=0$, it does not possess a three-dimensional inverse. It does, however, possess a two-dimensional inverse, which can be uniquely written as [30]

$$\boldsymbol{k}_c^{-2}=(\boldsymbol{k}_c^2\,{}^\times_\times\,\boldsymbol{uu})/\mathrm{spm}(\boldsymbol{k}_c^2). \tag{11}$$

The double-cross product of two dyadics is defined through $(\boldsymbol{ab})\,{}^\times_\times\,(\boldsymbol{cd})=(\boldsymbol{a}\times\boldsymbol{c})(\boldsymbol{b}\times\boldsymbol{d})$ and spm( ) is the two-dimensional determinant function ('sum of principal minors' of the three-dimensional dyadic) defined by $\mathrm{spm}\,\boldsymbol{A}=\boldsymbol{A}\,{}^\times_\times\,\boldsymbol{A}:\boldsymbol{I}/2$. That (11) is really valid can be checked by writing $\boldsymbol{k}_c^2$ in component form. Because a symmetric dyadic always possesses three orthogonal eigenvectors, we can write the two-dimensional dyadic $\boldsymbol{\epsilon}$ as

$$\boldsymbol{\epsilon}=\epsilon_v\boldsymbol{vv}+\epsilon_w\boldsymbol{ww} \tag{12}$$

with $\boldsymbol{u},\boldsymbol{v},\boldsymbol{w}$ an orthonormal system of unit vectors. Inserting (12) in (10) we have

$$\boldsymbol{k}_c^2=k_{cv}^2\boldsymbol{vv}+k_{cw}^2\boldsymbol{ww}\quad\text{with}\quad k_{ci}^2=\omega^2\mu\epsilon_i-\beta^2,\quad i=v,w. \tag{13}$$

Hence, (11) gives us

$$\boldsymbol{k}_c^{-2}=k_{cv}^{-2}\boldsymbol{vv}+k_{cw}^{-2}\boldsymbol{ww}. \tag{14}$$

To obtain the equations for the longitudinal fields we substitute (8), (9) in (4), (5)

$$\nabla\cdot\left((\boldsymbol{k}_c^{-2}\,{}^\times_\times\,\boldsymbol{uu})\cdot(\beta\boldsymbol{u}\times\nabla e+\omega\mu\nabla h)\right)+\omega\mu h=0 \tag{15}$$

$$\nabla\cdot\left(\boldsymbol{k}_c^{-2}\cdot(\omega\boldsymbol{\epsilon}\cdot\nabla e-\beta\boldsymbol{u}\times\nabla h)\right)+\omega\epsilon_u e=0. \tag{16}$$

Equations (15) and (16) constitute a pair of equations which are going to apply in our analysis. The operator L operates on the pair of scalar functions (e,h), which we denote by f in our abstract linear space. Defining the inner product (.,.) by

$$(f_1,f_2)=\int(e_1,h_1)\begin{pmatrix}e_2\\h_2\end{pmatrix}dS \tag{17}$$

where the integration extends over the whole $x-y$ plane, we have to define the explicit form of the operator L in such a way that it is self-adjoint with respect to the inner product (17). As boundary conditions, we take exponential decay of the fields e and h as $\rho\to\infty$, because only such guided solutions are of interest to us for the moment. It can be readily demonstrated that the definition

$$Lf=\begin{pmatrix}\omega\nabla\cdot(\boldsymbol{k}_c^{-2}\cdot\boldsymbol{\epsilon}\cdot\nabla e)+\omega\epsilon_u e-\beta\nabla\cdot(\boldsymbol{k}_c^{-2}\cdot\boldsymbol{u}\times\nabla h)\\ \beta\nabla\cdot\left((\boldsymbol{k}_c^{-2}\,{}^\times_\times\,\boldsymbol{uu})\cdot(\boldsymbol{u}\times\nabla e)\right)+\omega\mu\nabla\cdot\left((\boldsymbol{k}_c^{-2}\,{}^\times_\times\,\boldsymbol{uu})\cdot\nabla h\right)+\omega\mu h\end{pmatrix} \tag{18}$$

leads to a self-adjoint operator. In fact, we can evaluate

$$\begin{aligned}(f_1,Lf_2)=\int\Big(&-\omega\nabla e_1\cdot(\boldsymbol{k}_c^{-2}\cdot\boldsymbol{\epsilon})\cdot\nabla e_2\\&+\omega\epsilon_u e_1e_2-\omega\mu\nabla h_1\cdot(\boldsymbol{k}_c^{-2}\,{}^\times_\times\,\boldsymbol{uu})\cdot\nabla h_2\\&+\omega\mu h_1h_2-\beta\nabla h_2\cdot\boldsymbol{u}\times(\boldsymbol{k}_c^{-2})\cdot\nabla e_1\\&-\beta\nabla h_1\cdot\boldsymbol{u}\times\boldsymbol{k}_c^{-2}\cdot\nabla e_2\Big)\,dS\end{aligned} \tag{19}$$

when we note that the divergence terms, reduced to line integrals at infinity, does not contribute because of the assumed exponential decay of the fields.

To be self-adjoint, the operator L in (19) should give an expression symmetric in 1 and 2. If ϵ is a symmetric dyadic, as presumed, we can readily check that every term in (19) is symmetric except for the last two, which, however, form a symmetric pair. So, L is self-adjoint and we can apply the functional equation (2).

The eigenvalue equation $Lf = 0$ is from the definition (18) clearly of nonstandard form for the visible parameters ω, β and any anisotropic parameters hidden in the dyadic ϵ. Also, all geometrical parameters that may appear in the functional relation $\epsilon(\rho)$ are certainly nonlinear in the operator L. The reason is mainly the dyadic function $\boldsymbol{k}_c^{-2}$, which contains all these parameters in a very complicated fashion. In fact, (2) can be written in the form

$$\int \Big\{ \omega\big[\epsilon_u e^2 + \mu h^2 - \nabla e\cdot \boldsymbol{k}_c^{-2}\cdot\epsilon\cdot\nabla e - \mu(\boldsymbol{u}\times\nabla h)\cdot\boldsymbol{k}_c^{-2}\cdot(\boldsymbol{u}\times\nabla h)\big] + 2\beta(\boldsymbol{u}\times\nabla h)\cdot\boldsymbol{k}_c^{-2}\cdot\nabla e\Big\}\, dS = 0 \qquad (20)$$

from which no parameter can be explicitly solved unless ϵ is constant, which is not the case for a guiding structure.

Now we might try to define new parameters out of the old ones to obtain a simpler functional relationship for some of them. In fact, if instead of ω and β we consider ω^2 and $v_p = \omega/\beta$ for new independent parameters, we see that (20) is a linear equation in the parameter ω^2 and can be solved to give

$$\omega^2 = \frac{\int\big[\nabla e\cdot \boldsymbol{M}\cdot\epsilon\cdot\nabla e + (\boldsymbol{u}\times\nabla h)\cdot\boldsymbol{M}\cdot\mu(\boldsymbol{u}\times\nabla h) - 2(\boldsymbol{u}\times\nabla h)\cdot\boldsymbol{M}\cdot\nabla e\big]\, dS}{\int\left(\epsilon_u e^2 + \mu h^2\right) dS} \qquad (21)$$

where we denote

$$\boldsymbol{M} = \omega^2\boldsymbol{k}_c^{-2} = \left(\mu\epsilon_v - v_p^{-2}\right)^{-1}\boldsymbol{vv} + \left(\mu\epsilon_w - v_p^{-2}\right)^{-1}\boldsymbol{ww}. \qquad (22)$$

The dispersion relation will now be obtained in the form $\omega^2 = f(v_p)$, from which it is not difficult to calculate the result in the form $\omega = f(\beta)$.

The approximative calculation of a point on the dispersion curve is started from a given value of v_p, after which the field functions e, h are approximated by suitable trial functions f and g, respectively, containing a few free parameters. The only condition for the choice of the functions f, g is continuity. In fact, if there is a discontinuity in f or g, the gradient operation gives us delta functions, which appear squared in the functional and as such are meaningless because the factor of a delta function must be continuous. Since (21) is a stationary functional, we could apply the well-known Rayleigh–Ritz method where these parameters appear as linear coefficients in f and g, in which case we obtain a set of linear equations for the coefficients by differentiating (21) with respect to these parameters and setting the derivatives equal to zero. However, we also might choose parameters in the functions f, g in nonlinear fashion, in which case the stationary point of (21) is found by observing values of the functional. Because the field outside the fiber can best be approximated applying exponential functions with parameters in the exponent, this latter method is very suitable to the open waveguide problem. However, the number of parameters must not be very great. On the other hand, only a modest computer or programmable calculator is sufficient for the analysis.

The functional (21) was derived without weak guidance assumption, whence its application is not limited to optical fibers. Also, no assumption of perturbational anisotropy was ever made. In this manner, (21) appears to be the most general functional for transversely anisotropic waveguides, and to the knowledge of the authors has not been presented before.

In the literature, finite-element method (FEM) together with the Rayleigh–Ritz optimization or some other discrete technique is generally applied for dielectric waveguide analysis, leading to a large-dimension set of linear equations [12], [15], [23], [26], [31]–[36]. Nonlinear optimizable parameters in a variational method were recently applied to circularly symmetric isotropic graded-index fibers in scalar theory [37]. When comparing our method with FEM, one further advantage is seen. It is widely observed, that FEM and Rayleigh–Ritz give rise to unphysical solutions called spurious modes, which seem to be inherent to the approximate method [12]. Such modes do not appear when applying direct observation of the functional (21) and trial functions which are known to be physical. To find out whether the solution is spurious or not, with the FEM method, a large number of points must be calculated, which further widens the difference in computer capacity required by these two methods.

III. Testing the Functional: The Isotropic Step-Index Fiber

To obtain an idea of the accuracy of the functional (21), we first apply it to the weakly guiding isotropic step-index fiber, which has been thoroughly analyzed by many authors, [38], [39], for example. For the general isotropic dielectric waveguide, the functional takes on the simplified form

$$\omega^2 = \frac{\int\left(\mu\epsilon - v_p^{-2}\right)^{-1}\left(\epsilon(\nabla e)^2 + \mu(\nabla h)^2 - \frac{2}{v_p}\boldsymbol{u}\cdot\nabla h\times\nabla e\right) dS}{\int\left(\epsilon e^2 + \mu h^2\right) dS} \qquad (23)$$

where $\epsilon(\rho)$ is a scalar function. As trial functions we may take any continuous functions e, h.

For a weakly guiding step-index fiber, (23) can be further simplified. In fact, if the medium in the core is denoted by 1 and in the cladding by 2, we can define the parameters 'normalized frequency' V and 'normalized propagation factor' b by

$$V=\sqrt{k_1^2-k_2^2}\,a=\sqrt{\Delta}\,k_2 a \tag{24}$$

$$b=\frac{\beta^2-k_2^2}{k_1^2-k_2^2}=\frac{\beta^2-k_2^2}{V^2}a^2. \tag{25}$$

The quantity

$$\Delta=\frac{k_1^2-k_2^2}{k_2^2}=\frac{\epsilon_1-\epsilon_2}{\epsilon_2} \tag{26}$$

is much smaller than unity, typically less than 1 percent in an optical fiber. The dielectric function can be written concisely as

$$\epsilon(\rho)=\epsilon_2(1+\Delta P(\rho)) \tag{27}$$

where $P(\rho)=1$ for $\rho<a$, and $=0$ for $\rho>a$, for a step-index guide. In the limit case $\Delta\to 0$, (23) can be seen to reduce to

$$V^2=\frac{\int\frac{a^2}{P(\rho)-b}\left(\sqrt{\epsilon_2}\,\nabla e-\sqrt{\mu}\,\boldsymbol{u}\times\nabla h\right)^2 dS}{\int\left(\epsilon_2 e^2+\mu h^2\right)dS} \tag{28}$$

which does not explicitly depend on the parameter Δ. This functional is very easy to apply. To approximate the basic mode denoted by HE_{11} with $\cos\phi$ or $\sin\phi$ dependence we may write

$$e(\rho,\phi)=f(\rho)\cos\phi \tag{29}$$

$$h(\rho,\phi)=Hf(\rho)\sin\phi \tag{30}$$

where H is a constant and $f(\rho)$ is a function approximating the true radial dependence of the fields.

The parameter H must be chosen so that (28) is stationary. Inserting (29) and (30) in (28) and setting the derivative of V^2 with respect to H equal to zero, gives us an equation for H. It is easy to find out that for any function $f(\rho)$, the optimum value for H is either $1/\eta_2$ or $-1/\eta_2$ with $\eta_2=\sqrt{\mu/\epsilon_2}$. The choice $H=-1/\eta_2$ gives us zero transverse fields on the axis corresponding to the EH_{11} mode, which is not of our interest. Hence, we take for the HE_{11} mode

$$H=1/\eta_2. \tag{31}$$

Substituting (29), (30), and (31) in (28) gives us the functional

$$V^2=\frac{\int\frac{a^2}{P(\rho)-b}\left(f'+\frac{f}{\rho}\right)^2\rho\,d\rho}{\int f^2\rho\,d\rho} \tag{32}$$

where the integration extends from 0 to ∞.

As a check we first insert the exact fields in the functional. The exact function is [40]

$$f_e(\rho)\begin{array}{ll}=J_1(u\rho/a)/J_1(u), & \text{for } \rho\leqslant a\\ =K_1(w\rho/a)/K_1(w), & \text{for } \rho\geqslant a\end{array} \tag{33}$$

where J and K denote the Bessel and modified Hankel functions, respectively, and

$$u=V\sqrt{1-b}$$
$$w=V\sqrt{b}. \tag{34}$$

When (33), (34) are substituted in the functional (32), after some operations on Bessel functions, the following equation is obtained:

$$\frac{J_0(u)}{uJ_1(u)}=\frac{K_0(w)}{wK_1(w)}. \tag{35}$$

This is the well-known eigenvalue equation for the HE_{11} mode [38], which is exact in the limit $\Delta=0$ for the weakly guiding step-index fiber.

Next, we study some approximate trial functions. In the core region, it is simple to choose a polynomial of odd degree with undetermined coefficients. In the cladding, the exponent function appears to be the most evident choice with a parameter in the exponent and with a possible $1/\sqrt{\rho}$ factor. Three different test functions were in fact attempted, each continuous at the core-cladding interface $\rho=a$

$$f_1(\rho)\begin{array}{ll}=\rho/a, & \rho\leqslant a\\ =\exp[-\gamma(\rho-a)], & \rho\geqslant a\end{array} \tag{36}$$

$$f_2(\rho)\begin{array}{ll}=(1-\alpha)\rho/a+\alpha(\rho/a)^3, & \rho\leqslant a\\ =\exp[-\gamma(\rho-a)], & \rho\geqslant a\end{array} \tag{37}$$

$$f_3(\rho)\begin{array}{ll}=(1-\alpha)\rho/a+\alpha(\rho/a)^3, & \rho\leqslant a\\ =\sqrt{a/\rho}\exp[-\gamma(\rho-a)], & \rho\geqslant a.\end{array} \tag{38}$$

The simplest function f_1 only involves one optimizable parameter γ, whereas f_2 and f_3 have two parameters α and γ. Because γ appears in nonlinear fashion, the optimization cannot be done analytically even in the simplest f_1 case. Stationary values of the functional (32), however, are easy to find with a simple computer or programmable calculator for accurate approximations of the dispersion relation $V=V(b)$.

Results for functions f_1, f_2, and f_3 compared with those for the exact function f_e (number 4) are given in Figs. 1, 2, and 3 and Table I. It is seen that above the value $b=0.1$ the accuracy is very good. For large values of b and V, f_1 gives largest errors (Table I contains the error for the V variable, the error for b is smaller), which is due to the fact that the fields are concentrated in the core and the linear approximation of f_1 is simply not good enough, whereas the cubic functions of f_2 and f_3 are very good. For low values of b, f_3 outweighs f_2 because the fields are now mainly in the cladding, where f_3 is a better approximation.

For values of b close to zero the functional does not work very well, because it has a singularity at $b=0$, Fig. 4.

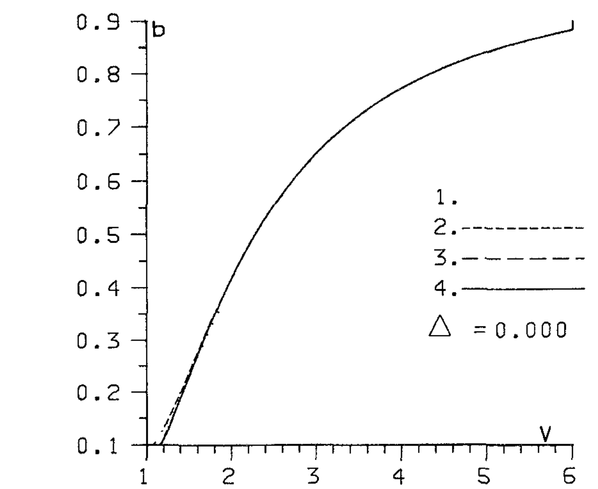

Fig. 1. Dispersion curve for a cylindrically symmetric step-index fiber in the weakly guiding limit $\Delta \rightarrow 0$. Numbers 1 to 3 refer to the test functions f_i defined in (36)–(38), and 4 to the exact function f_e in (33).

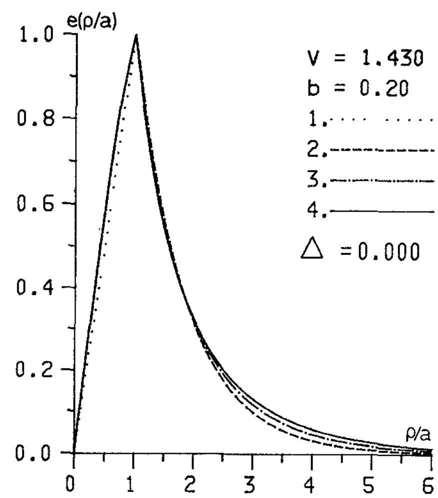

Fig. 2. Optimized field functions, f_i, $i=1$–3, and the exact function f_e (4) for the normalized frequency parameter $V=1.430$ in the weakly guiding limit $\Delta \rightarrow 0$.

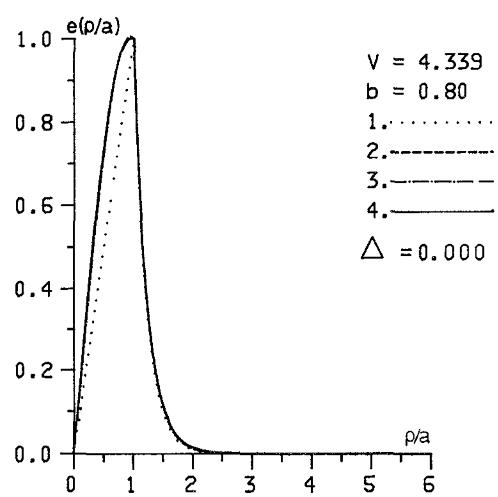

Fig. 3. Same as in Fig. 2 for $V=4.339$.

TABLE I
VALUES OF THE NORMALIZED FREQUENCY PARAMETER V FOR DIFFERENT VALUES OF THE NORMALIZED PROPAGATION FACTOR PARAMETER b AND THE CORRESPONDING ERROR FOR V IN PERCENT

	f_1		f_2		f_3		f_e	G	
b	V	%	V	%	V	%	V	V	%
.90	7.1898	9.160	6.5896	0.048	6.5896	-0.023	6.5865	6.6310	0.676
.80	4.6291	6.690	4.3399	0.025	4.3400	0.021	4.3388	4.3865	1.100
.60	2.8203	3.877	2.7145	-0.022	2.7153	0.007	2.7151	2.7714	2.073
.40	1.9898	1.991	1.9466	-0.226	1.9505	-0.023	1.9510	2.0024	2.634
.20	1.4168	-0.891	1.4023	-1.908	1.4252	-0.317	1.4296	1.4430	0.939

f_1, f_2, f_3 refer to different approximating functions, f_e is the exact function, and G refers to Gloge's approximative formula (40); $\Delta = 0$.

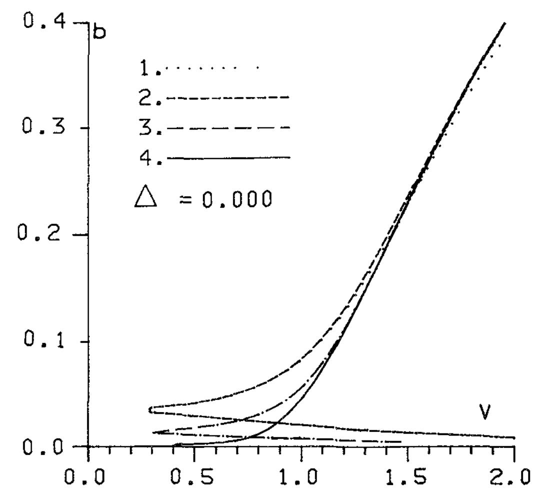

Fig. 4. Approximations (1,2,3) to the exact (4) dispersion relation for low parameter b, V values.

In fact, the relation $b(V)$ has an essential singularity at $V=0$, evident from the asymptotic evaluation of the correct solution at $V=0$ [41]

$$b \sim (2/\gamma V)^2 \exp\left(-(2/V)^2\right), \qquad \gamma = 1.781, \cdots \tag{39}$$

because all derivatives of b with respect to V can be seen to vanish at the origin. Instead of making new asymptotic approaches for the low b region, we exclude the range $b < 0.1$ from our study.

Greater accuracies could have been obtained for more complicated trial functions. However, one of the objectives was to evaluate a method applicable for simple computing devices, which limits the number of optimizable parameters.

The column G in Table I refers to the analytic approximation by Gloge [39] for the dispersion curve

$$b(V) = 1 - \left\{(1+\sqrt{2})/\left(1+(4+V^4)^{1/4}\right)\right\}^2 \tag{40}$$

which gives a fair accuracy for values $V > 1$.

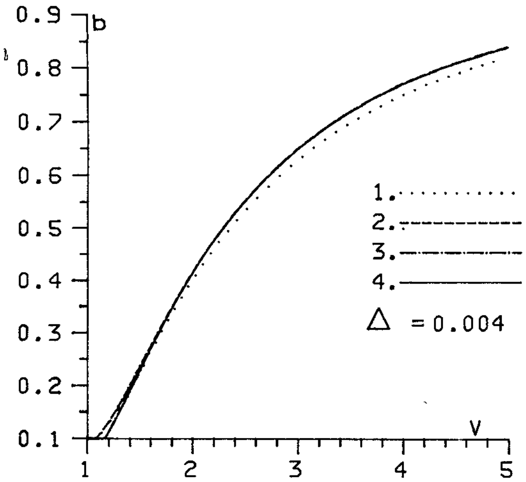

Fig. 5. Same as in Fig. 1 for Δ = 0.004.

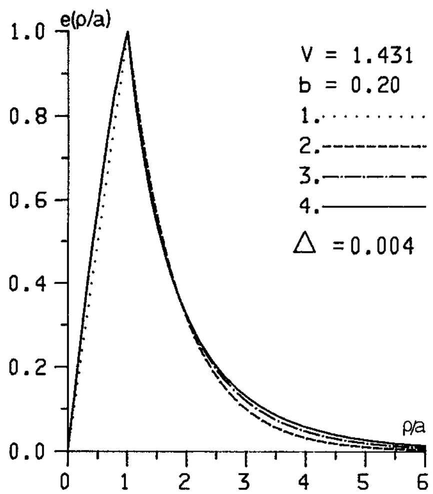

Fig. 6. Same as in Fig. 2 for Δ = 0.004.

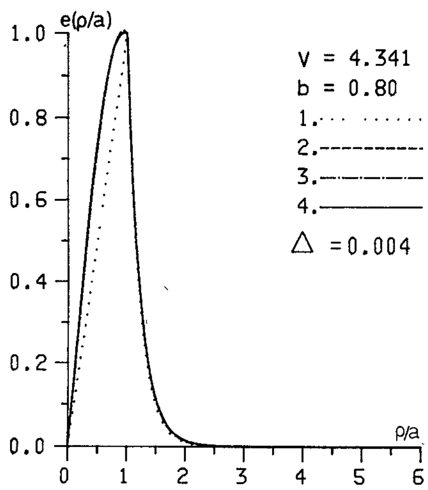

Fig. 7. Same as in Fig. 3 for Δ = 0.004.

TABLE II
VALUES OF THE NORMALIZED PARAMETER V FOR DIFFERENT VALUES OF THE NORMALIZED PROPAGATION PARAMETER b AND THE CORRESPONDING ERROR IN PERCENT.

	f_1		f_2		f_3		f_e
b	V	%	V	%	V	%	V
.90	7.1928	9.171	6.5917	0.047	6.5917	0.047	6.5886
.80	4.6318	6.701	4.3420	0.023	4.3420	0.025	4.3409
.60	2.8226	3.886	2.7164	-0.024	2.7172	0.005	2.7170
.40	1.9917	1.996	1.9483	-0.228	1.9522	-0.025	1.9527
.20	1.4185	-0.882	1.4038	-1.903	1.4266	-0.310	1.4311

f_1, f_2, f_3 refer to different approximating functions and f_e to the solution of the exact eigenvalue equation (41). $\Delta = 0.004$.

The test of the weakly guiding limit $\Delta \to 0$ of the cylindrically symmetric step-index fiber thus demonstrates the applicability of the present variational method and the asymptotic functional (28).

To test the more general functional (23), we take a nonzero value for the dielectric step parameter Δ, namely $\Delta = 0.004$. For the same test functions (29), (30) we approximate the parameter H by (31), which however, is not a strict optimum in this case. Optimization of H can be seen to lead to values differing from (31) very slightly and the error in the functional comes mainly from the choice of the function $f(\rho)$ for small values of Δ. Taking the same test functions f_i as in (36)–(38), we have the approximations depicted in Figs. 5, 6, and 7, and Table II. Number 4 denotes the exact values obtainable from the more general eigenvalue equation [39]

$$\frac{J_0(u)}{uJ_1(u)} = \left(1 - \frac{\Delta}{2}\right)\frac{K_0(w)}{wK_1(w)} \tag{41}$$

which is not exact, but more accurate than (35) when Δ is small.

It is seen that the accuracy is not much different from that of the previous example where $\Delta = 0$.

IV. Application to Anisotropic Fibers

To apply the functional (21) to optical fibers with transverse anisotropy, we consider two examples of weakly guiding step-index fibers with either anisotropic core or anisotropic core and cladding. These examples are simple first steps towards an analysis of more realistic fibers which are produced by the present technology. The functional (21) is able to handle all kinds of transverse anisotropies, not necessarily constant, and arbitrary inhomogeneities. The problem for the present is to obtain a reliable expression for the relation between the applied stress and the resulting dielectric anisotropy of the fiber material. It has been found that the anisotropy not only depends on the stress itself, but also on the method of preparation of the glass and on its thermal history [42], which makes the relation very complicated to express.

A. Circular Step-Index Fiber with Anisotropic Core and Isotropic Cladding

The dielectric dyadic is now assumed to be of the form

$$\epsilon = \epsilon_2 \left[(\boldsymbol{E} + \Delta P(\rho)\kappa) + (1 - \Delta P(\rho)) \boldsymbol{uu} \right] \tag{42}$$

where P is the same function as in (27) and κ is the constant dyadic

$$\kappa = A_v \boldsymbol{vv} + A_w \boldsymbol{ww}. \tag{43}$$

Δ is a parameter which is assumed to be small. Thus the medium is almost transversely isotropic with the dielectric factor ϵ_2, which is that of the medium in the cladding, but the core has a slightly different dyadic dielectric factor. We define two parameters V^2 and b in terms of Δ as follows:

$$V^2 = \Delta (k_2 a)^2 \tag{44}$$

$$b = (\beta^2 - k_2^2) a^2 / V^2. \tag{45}$$

These definitions coincide with (24), (25), if the parameter k_1 does not show because it is not unique here. The dyadic $\boldsymbol{M}$ in (22) can now be evaluated. In fact, we may write

$$\boldsymbol{k}_c^2 = (\kappa P - b\boldsymbol{E}) V^2 / a^2 \tag{46}$$

whence

$$\boldsymbol{M} = \omega^2 a^2 \boldsymbol{D} / V^2, \qquad \boldsymbol{D} = (\kappa P - b\boldsymbol{E})^{-1}. \tag{47}$$

Substituting (47) and (42) in (21), eliminating ω and letting $\Delta \to 0$, leaves us with the following simple functional for V^2:

$$V^2 = \frac{\int \left(\sqrt{\epsilon_2}\, \nabla e - \sqrt{\mu}\, \boldsymbol{u} \times \nabla h\right) \cdot \boldsymbol{D} \cdot \left(\sqrt{\epsilon_2}\, \nabla e - \sqrt{\mu}\, \boldsymbol{u} \times \nabla h\right) a^2 \, dS}{\int \left[\left(\sqrt{\epsilon_2}\, e\right)^2 + \left(\sqrt{\mu}\, h\right)^2 \right] dS} \tag{48}$$

The functional (28) is obviously the isotropic special case of the functional (48). The normalized propagation parameter b and the anisotropy parameters A_v, A_w are contained in the symmetric dyadic $\boldsymbol{D}$, which can be written more explicitly as

$$\boldsymbol{D} = (\kappa P - b\boldsymbol{E})^{-1} = \frac{\boldsymbol{vv}}{A_v P - b} + \frac{\boldsymbol{ww}}{A_w P - b} = \begin{cases} \boldsymbol{vv}/(A_v - b) + \boldsymbol{ww}/(A_w - b), & \rho < a \\ -\boldsymbol{E}/b, & \rho > a. \end{cases} \tag{49}$$

Now we are ready to apply (48) by inserting suitable trial functions and finding the stationary points. First we try the functions (29), (30), and put $H = 1/\eta_2$. The angle ϕ is measured from the $\boldsymbol{v}$-direction. We have

$$\sqrt{\epsilon_2}\, \nabla e - \sqrt{\mu}\, \boldsymbol{u} \times \nabla h = \sqrt{\epsilon_2} \left(\frac{f}{\rho} + f' \right) \boldsymbol{v} \tag{50}$$

which inserted in (48) shows us that in this approximation, the functional is the same as that for the isotropic fiber (32), with $A_v P(\rho)$ instead of $P(\rho)$. This can also be interpreted in such a way that if the dispersion relation for the

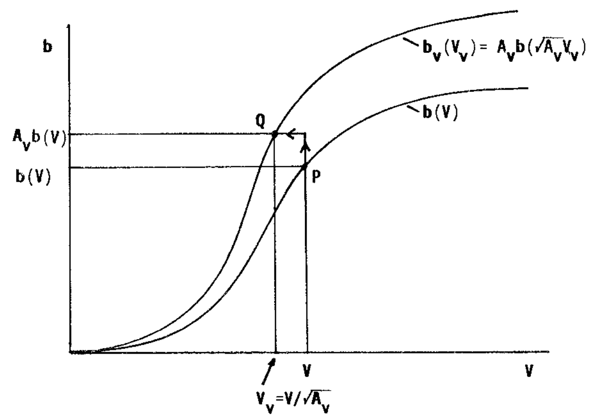

Fig. 8. Construction of the dispersion curve for the slightly anisotropic weakly guiding fiber in terms of the dispersion curve for the isotropic fiber. Every point P of the isotropic curve is mapped onto a point Q of the anisotropic curve.

isotropic step-index fiber is $V^2 = f(b)$, in this approximation we have for the anisotropic fiber

$$V^2 = \frac{1}{A_v} f(b/A_v). \tag{51}$$

The transformation (51) has the effect of shifting the isotropic dispersion curve as shown in Fig. 8.

Rotating the test function in the $\boldsymbol{v}$-, $\boldsymbol{w}$-plane by 90° gives us (49) with $\boldsymbol{w}$ instead of $\boldsymbol{v}$ and (51), with A_w instead of A_v. Thus the dispersion relations are different for the two polarizations. It is noted that there was no assumption of smallness of the anisotropy, but the error involved in the isotropic test function applied here is probably larger for greater anisotropy.

The birefringence concept was originally defined for two modes with dispersion characteristics close to one another. The question was to separate two degenerate modes in a circularly symmetric isotropic fiber by means of a perturbation of some kind. The concept is not very useful for modes whose dispersion characteristics differ very much from each other. Thus for a small anisotropy, the birefringence can be well calculated using the isotropic test functions. In the general case, we can write for the two polarizations

$$B = 2\frac{\beta_v a - \beta_w a}{\beta_v a + \beta_w a} = 2\frac{\sqrt{b_v + 1/\Delta} - \sqrt{b_w + 1/\Delta}}{\sqrt{b_v + 1/\Delta} + \sqrt{b_w + 1/\Delta}} \approx \frac{\Delta}{2}(b_v - b_w). \tag{52}$$

The last expression is valid for $\Delta \to 0$, if b_v, b_w are not very small. If there only is anisotropy in the $\boldsymbol{v}$-direction, $b_w = b$ the isotropic value, we see that the birefringence is proportional to the separation in the dispersion curves of the anisotropic and isotropic cases. Moreover, we see that the birefringence is proportional to Δ and not Δ^2, as would be the case for an isotropic perturbed guide. This fact was earlier demonstrated by many authors applying perturbational analysis and perturbational coupled-wave analysis, [6], [7]. For a perturbational anisotropy, (52) can be written

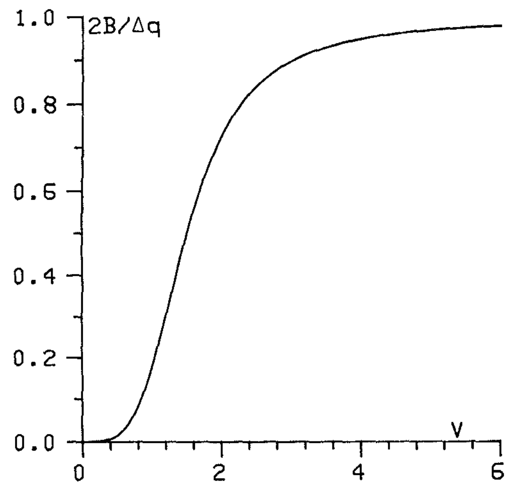

Fig. 9. Normalized birefringence $2B/\Delta q$ for the step-index fiber with anisotropic core and isotropic cladding in the limit of weak guidance and perturbational anisotropy.

for $A = 1 + q$

$$B \approx \frac{\Delta q}{2}\left(b(V) + \frac{1}{2}Vb'(V)\right) \tag{53}$$

where b' denotes the derivative of b with respect to V. Applying (40), the function of V in brackets can be sketched as in Fig. 9. It is seen that the birefringence increases monotonically with increasing values of the parameter V.

For large values of V, B can be approximated by $\Delta q/2$. As an example, for a practical value of the birefringence $B = 10^{-4}$ at $V = 2.4$, we have from Fig. 9 $\Delta q = 2.3 \cdot 10^{-4}$, whence for $\Delta = 0.01$ we must have $q = 0.023$.

B. Circular Step-Index Fiber with Anisotropic Core and Cladding

As a second example we consider a step-index anisotropic fiber with the dyadic parameter

$$\epsilon = \epsilon_2(1 + \Delta P(\rho))(\kappa + uu) \tag{54}$$

and the same definitions for the symbols as in the previous example. This time, the fiber is fabricated on an anisotropic cladding material, and the anisotropy is the same in the core.

Unlike in the previous example, the functional cannot be simplified in a form corresponding to (48). Hence, we must work with the general functional (21). Writing

$$\epsilon_v = \epsilon_2(1 + \Delta P(\rho))A_v \tag{55}$$

$$\epsilon_w = \epsilon_2(1 + \Delta P(\rho))A_w \tag{56}$$

we substitute (22) in (21). Applying (29), (30), (31), and (38) for the trial function, optimizing the parameters α and γ, we have the dispersion relations shown in Figs. 10 and 11. It is seen that the effect of the parameter Δ is much less pronounced than in the case A. This is easily understood from the difference of the definitions (42) and (54). In fact, taking $A_w = 1$ and $A_v = 1 + q$, it is seen that in (42) the anisotropic parameter q appears in the term $q\Delta P\epsilon_{2}vv$, whereas in (54) the corresponding term is $q(1 + \Delta P)\epsilon_2 vv$, which does not vanish for $\Delta = 0$. This means that the term

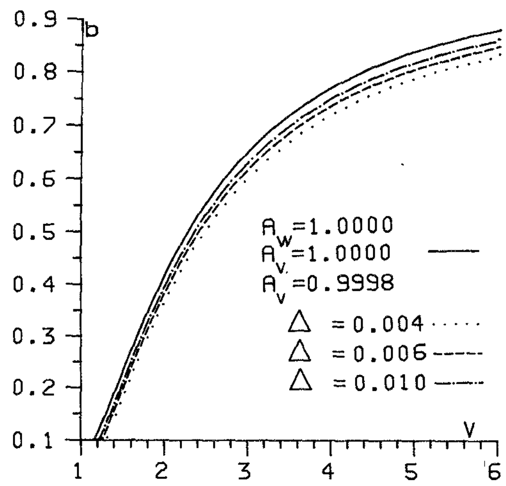

Fig. 10. Dependence of the dispersion relation on the dielectric parameter Δ for the anisotropic parameter $A = 0.9998$.

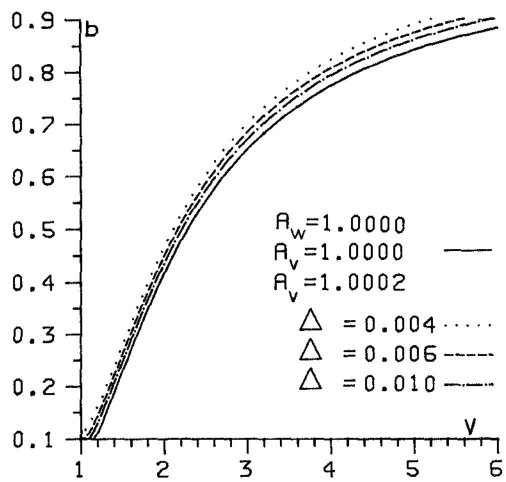

Fig. 11. Same as in Fig. 10 for $A = 1.0002$.

$q\Delta$ is replaced by q in many contexts for weakly guiding fibers, and thus Δ has a minor effect on the propagation properties.

The same can also be seen from an asymptotic consideration of the birefringence parameter B, (52). If we approximate for low anisotropy the ratio of the propagation factors β_v/β_w by $\sqrt{1+q}$, which corresponds to the ratio for plane waves polarized in the w- and v-directions, we have

$$B \approx q/2 \tag{57}$$

which does not depend on the parameter Δ.

Calculations from the functional for low values of Δ and q (around $10^{-3} - 10^{-4}$) show that B defined by (57) is a valid approximation for values of V between 1 and 6 with less than a 1-percent error.

V. Conclusion

Applying the theory of nonstandard eigenvalue problems and variational principles, a stationary functional for dielectric open waveguides with transverse anisotropic dielectric tensor was constructed. The functional was tested for isotropic well-known step-index circular fibers and was seen to give results for two-parameter test functions with less than 1 percent of error in the interesting range of frequencies. Further, the functional was applied for two types of anisotropic optical fibers: one with anisotropic core and other with a both core and cladding anisotropic. For low anisotropy and weak guidance, approximate expressions for the birefringence of the two HE_{11} modes were seen to result in analytic form. The method seems applicable to more complicated problems with more parameters in the test functions. In the present form, however, a computer of very modest capacity or even a programmable calculator is sufficient.

Acknowledgment

Discussions with Mr. J. Saijonmaa from the Telecommunication Laboratory and Mr. J. Kurki from the Electron Physics Laboratory, Helsinki University of Technology, are thankfully acknowledged.

References

[1] W. O. Schlosser, "Delay distortion in weakly guiding optical fibers due to elliptic deformation of the boundary," *Bell Syst. Tech. J.*, vol. 51, no. 2, pp. 487–492, Feb. 1972.
[2] F. P. Kapron, N. F. Borrelli, and D. B. Keck, "Birefringence in optical waveguides," *IEEE J. Quantum Electron.*, vol. QE-8, no. 2, pp. 222–225, Feb. 1972.
[3] V. Ramaswamy and W. G. French, "Influence of noncircular core on the polarisation performance of single mode fibres," *Electron. Lett.*, vol. 14, no. 5, pp. 143–144, Mar. 1978.
[4] V. Ramaswamy, W. G. French, and R. D. Standley, "Polarization characteristics on noncircular core single-mode fibers," *Appl. Opt.*, vol. 17, no. 18, pp. 3014–3017, Sept. 1978.
[5] V. Ramaswamy, R. D. Standley, D. Sze, and W. G. French, "Polarization effects in short length, single mode fibers," *Bell. Syst. Tech. J.*, vol. 57, no. 3, pp. 635–651, Mar. 1978.
[6] M. J. Adams, D. N. Payne, and C. M. Ragdale, "Birefringence in optical fibres with elliptical cross-section," *Electron. Lett.*, vol. 15, no. 10, pp. 298–299, May 1979.
[7] J. D. Love, R. A. Sammut, and A. W. Snyder, "Birefringence in elliptically deformed optically fibres," *Electron. Lett.*, vol. 15, no. 20, pp. 615–616, Sept. 1979.
[8] R. B. Dyott, J. R. Cozens, and D. G. Morris, "Preservation in optical-fibre waveguides with elliptical cores," *Electron. Lett.*, vol. 15, no. 13, pp. 380–382, June 1979.
[9] D. N. Payne, A. J. Barlow, and J. J. Ramskov Hansen, "Development of low- and high-birefringence optical fibers," *IEEE Trans. Microwave Theory Tech.*, vol. MTT-30, no. 4, pp. 323–334, Apr. 1982.
[10] R. A. Sammut, "Birefringence in graded-index monomode fibres with elliptical cross-section," *Electron. Lett.*, vol. 16, no. 4, pp. 156–157, Feb. 1980.
[11] I. Kaminow, "Polarization in optical fibers," *IEEE J. Quantum Electron.*, vol. QE-17, no. 1, pp. 15–22, Jan. 1981.
[12] T. Okoshi, "Single-polarization single-mode optical fibers," *IEEE J. Quantum Electron.*, vol. QE-17, no. 6, pp. 879–884, June 1981.
[13] V. Ramaswamy, I. P. Kaminow, P. Kaiser, W. G. French, "Single polarization optical fibers: Exposed cladding technique," *Appl. Phys. Lett.*, vol. 33, no. 9, pp. 814–816, Nov. 1978.
[14] T. Katsuyama, H. Matsumura, and T. Suganuma, "Low-loss single polarization fibres," *Electron. Lett.*, vol. 17, no. 13, pp. 473–474, June 1981.
[15] Y. Namihira, Y. Ejiri, and K. Mochizuki, "Birefringence in elliptical-cladding single-polarization fibres," *Electron. Lett.*, vol. 18, no. 2, pp. 89–91, Jan. 1982.
[16] N. Imoto, N. Yoshizawa, J. I. Sakai, and H. Tshuhiya, "Birefringence in single-mode optical fiber due to elliptical core deformation and stress anisotropy," *IEEE J. Quantum Electron.*, vol. QE-16, no. 11, pp. 1267–1271, Nov. 1980.
[17] J. I. Sakai and T. Kimura, "Polarization behavior in multiply perturbed single-mode fibers," *IEEE J. Quantum Electron.*, vol. QE-18, no. 1, pp. 59–65, Jan. 1982
[18] F. J. Rosenbaum, "Hybrid modes on anisotropic dielectric rods," *IEEE J. Quantum Electron*, vol. QE-1, no. 9, pp. 367–374, Dec. 1965.
[19] S. Wang, M. L. Shah, and J. D. Crow, "Wave propagation in thin-film optical waveguides using gyrotropic and anisotropic materials and substrates," *IEEE J. Quantum Electron.*, vol. QE-8, no. 2, pp. 212–216, Feb. 1972.
[20] D. K. Paul and R. K. Shevgaonkar, "Multimode propagation in anisotropic optical waveguides," *Radio Sci.*, vol. 16, no. 4, pp. 525–533, July–Aug. 1981.
[21] A. Tonning "Circularly symmetric optical waveguide with strong anisotropy," *IEEE Trans. Microwave Theory Tech.*, vol. MTT-30, no. 5, pp. 790–794, May 1982.
[22] D. Marcuse, "Coupled-mode theory for anisotropic optical waveguides," *Bell Syst. Tech. J.*, vol. 54, no. 6, pp. 985–995, July–Aug. 1975.
[23] P. Vandenbulcke and P. E. Lagasse, "Eigenmode analysis of anisotropic optical fibres or integrated optical waveguides," *Electron. Lett.*, vol. 12, no. 5, pp. 120–122, Mar. 1976.
[24] J. R. Cozens: "Propagation in cylindrical fibres with anisotropic crystal cores," *Electron. Lett.*, vol. 12, no. 16, pp. 413–415, Aug. 1976.
[25] B. B. Chaudhury, "Wave propagation through weakly anisotropic straight and curved rectangular dielectric optical guides," *IEEE Trans. Microwave Theory Tech.*, vol. MTT-28, no. 3, pp. 231–234, Mar. 1980.
[26] N. Mabaya, P. E. Lagasse, and P. Vandenbulcke, "Finite element analysis of optical waveguides," *IEEE Trans. Microwave Theory Tech*, vol. MTT-29, no 6, pp. 600–605, June 1981.
[27] I. V. Lindell, "Variational methods for nonstandard eigenvalue problems in waveguide and resonator analysis," *IEEE Trans. Microwave Theory Tech.*, vol. MTT-30, no. 8, pp. 1194–1204, Aug. 1982.
[28] R. F. Harrington, *Time-Harmonic Electromagnetic Fields*. New York: McGraw-Hill, 1961, ch. 7.
[29] I. V. Lindell and A. H. Sihvola: "Variational analysis of a dielectrically loaded corrugated waveguide," in *Proc. 12th European Microwave Conf.*, Helsinki, Finland, 1982, pp. 312–316.
[30] I. V. Lindell, "Elements of dyadic algebra and its application in electromagnetics," Helsinki University of Technology, Radio Laboratory, Report S 126, 1981 (available from the author).
[31] C. Yeh, S. B. Dong, and W. Oliver, "Arbitrarily shaped inhomogeneous optical fibre or integrated optical waveguides," *J. Appl. Phys.*, vol. 46, no. 5, pp. 2125–2129, May 1975.
[32] C. Yeh, K. Ha, S. B. Dong, and W. B. Brown, "Single-mode optical waveguides," *Appl. Opt*. vol. 18, no. 10, pp. 1490–1504, May 1979.
[33] E. Yamashita, K. Atsuki, O. Hashimoto, and K. Kamijo, "Modal analysis of homogeneous optical fibers with deformed boundaries," *IEEE Trans. Microwave Theory Tech.*, vol. MTT-27, no. 4, pp. 352–356, Apr. 1979.
[34] K. Oyamada and T. Okoshi, "Two-dimensional finite-element method calculation of propagation characteristics of axially nonsymmetrical optical fibers," *Radio Sci.*, vol. 17, no. 1, pp. 109–116, Jan.–Feb. 1982.
[35] P. L. Chu, P. Y. Chen, and R. A. Sammut, "Finite-element analysis of birefringence in azymuthally inhomogeneous optical fibre," *Electron. Lett.*, vol. 18, no. 11, pp. 441–442, May 1982.
[36] R. Mittra, Y. L. Hoy, and V. Jamnejad, "Analysis of open dielectric wave-guides using mode-matching technique and variational methods," *IEEE Trans. Microwave Theory Tech.*, vol. MTT-28, no. 1, pp. 36–43, Jan. 1980.
[37] A. Sharma, S. I. Hosain, and A. K. Ghatak, "The fundamental mode of graded-index fibers: Simple and accurate variational methods," *Optical and Quantum Electron.*, vol. 14, no. 1, pp. 7–15, Jan. 1982.
[38] A. W. Snyder, "Asymptotic expressions for eigenfunctions and eigenvalues of a dielectric or otpical waveguide," *IEEE Trans. Microwave Theory Tech.*, vol. MTT-17, no. 12, pp. 1130–1138, Dec. 1969.
[39] D. Gloge, "Weakly guiding fibers," *Appl. Opt.*, vol. 10, no. 10, pp. 2252–2258, Oct. 1971.
[40] M. J. Adams, "*An Introduction to Optical Waveguides*," New York: Wiley, 1981.
[41] S. A. Schelkunoff, *Electromagnetic Waves*, Princeton, NJ: Van Nostrand, 1943, p. 428.

[42] N. Lagakos, R. Mohr, and O. H. El-Bayomi, "Stress optic coefficient and stress profile in optical fibers," *Appl. Opt.*, vol. 20, no. 13, pp. 2309–2313, July 1981.

Ismo V. Lindell (S'68–M'70–SM'83), for a photograph and biography please see page 526 the July 1983 issue of this TRANSACTIONS.

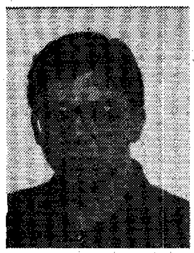

Markku I. Oksanen (S'81) was born in Jyväskylä, Finland on Dec. 1. 1958. He received the Dipl. Eng. degree in 1983 in electrical engineering from the Helsinki University of Technology, Espoo, Finland.

His main interest is in electromagnetic theory.

An Implantable Electric-Field Probe of Submillimeter Dimensions

T. E. BATCHMAN, SENIOR MEMBER, IEEE, AND GEORGE GIMPELSON, MEMBER, IEEE

***Abstract*—Many areas of biological research await the development of practical electric (*E*)-field probes with submillimeter dimensions for *in situ* measurements of RF electromagnetic fields. This paper reports on the design, fabrication, and testing of such a probe. The probe consists of a 0.6-mm dipole antenna, a zero-bias Schottky barrier diode and a unique highly resistive output lead structure. Experimental results indicate the probe does not perturb the field under investigation and is linear over a range of field strengths from less than 60 to over 1200 V/m. The probe has been designed so as to be independent of the media in which measurements are being made.**

I. INTRODUCTION

IN THE MID-1970's a series of articles appeared in the *New Yorker*, written by Paul Brodeur [1], which brought to the public's attention the present controversy over the question of what constitutes a safe level of electromagnetic radiation. The debate now centers around the criteria used by the U.S. to establish an exposure limit. Initially, it was assumed that only the thermal effects were hazardous, and so all that needed to be considered was the rate at which the human body dissipated the thermal energy.

However, in the last 15 years an impressive amount of evidence has been accumulated which demonstrates the existence of "nonthermal" effects [2]–[5]. In the late 1960's, Dr. W. R. Adey (then with the Brain Research Institute of UCLA) and A. H. Frey of Randomline, Inc., advanced theories on the biological effects of very low intensity microwaves, and collected experimental evidence for theoretical verification [6]. In the early 1970's Dr. K. V. Sudakov at P. K. Anokhin Institute in Moscow induced profound EEG and behavioral changes in mice using ELF modulated microwaves. Dr. R. Carpenter of the Bureau of Radiological Health is presently attempting to determine if there is a correlation between the formation of cateracts and microwave exposure. This concern over the effects of low-level non-ionizing radiation has led to a demand for more accurate methods of measuring electromagnetic fields within biological media.

Currently, there are three methods available for determining the strength of internal electromagnetic fields: the electric (E)-field probe, thermography, and the temperature probe. A comparison of these three internal dosimetric techniques has been made by H. Bassen *et al.*, [7] and it was noted that the E-field probe measurement is the only technique which directly monitors the electric field. Consequently, it neither depends on observed secondary effects nor assumes that all the internally deposited energy is transformed to heat. Both the temperature probe and thermography require a knowledge of the mass density and specific heat of the investigated region to determine the specific absorption rate. Furthermore, the sensitivity of these two methods is not great enough to allow for dosimetry at incident power densities of less than 10 mW/cm^2, as is often needed for low-intensity microwave research. The E-field probe does not suffer from these limitations, and has the advantage of continuous line scan capability and media independence.

Manuscript received February 7, 1983; revised May 4, 1983. This work was supported by the National Science Foundation.
T. E. Batchman is with the Department of Electrical Engineering, University of Virginia, Charlottesville, VA.
G. Gimpelson is with Harris Semiconductor, Melbourne, FL.

0018-9480/83/0900-0745$01.00 ©1983 IEEE